



ELSEVIER

Contents lists available at ScienceDirect

Chinese Chemical Letters

journal homepage: www.elsevier.com/locate/ccllet

Continuous-flow enzymatic synthesis of chiral lactones in a three-dimensional microfluidic reactor

Xuelel Deng^{a,1}, Meng Fan^{a,1}, Miao Wu^b, Xiaoyan Zhang^a, Ya Cheng^b, Jianye Xia^c, Yingping Zhuang^a, Weiping Zhu^a, Xuhong Qian^a, Yunpeng Bai^{a,*}

^a State Key Laboratory of Bioreactor Engineering, Shanghai Collaborative Innovation Center for Biomanufacturing, East China University of Science and Technology, Shanghai 200237, China

^b The Extreme Optoelectromechanics Laboratory, School of Physics and Materials Science, East China Normal University, Shanghai 200241, China

^c Tianjin Institute of Industrial Biotechnology, Chinese Academy of Sciences, Tianjin 300308, China

ARTICLE INFO

Article history:

Received 8 March 2023

Revised 7 June 2023

Accepted 13 June 2023

Available online 16 June 2023

Keywords:

Continuous-flow

Flow chemistry

Microreactor

Biocatalysis

Carbonyl reductase

Asymmetric reduction

ABSTRACT

A new continuous-flow process for the enzymatic synthesis of optically pure γ -lactones, which are used as flavors and fragrances in the food and cosmetic industries, was developed in a three-dimensional microfluidic reactor. The microchannels (175 mm in length, 0.9 mm in depth, and 1.72 mL in volume) were carved precisely inside a single borosilicate glass (90 mm \times 75 mm \times 12 mm) with ultrafast femtosecond laser micromachining. The flow field analysis and reaction simulation showed that the mixing of substrates and enzymes was enhanced, allowing the adjustment of residence time in a wide window. SmCR_{V4}, a carbonyl reductase with excellent catalytic activity and enantioselectivity toward γ/δ -keto acids, was employed for the asymmetric synthesis of various chiral lactones. 30 mmol/L (*R*)- γ -decalactone (**3g**) can be obtained in 26 s with a space-time yield (STY) up to 16,877 g L⁻¹ d⁻¹, which is 14.4 times higher than the highest STY of batch reaction reported previously. This continuous-flow process was applied to the synthesis of 6 chiral lactones. In addition, the scaled-up synthesis of **3g** was carried out in 6 cascade microreactors continuously for 6 h, demonstrating the feasibility and stability of the 3D continuous-flow process in enzymatic synthesis of optically pure compounds.

© 2023 Published by Elsevier B.V. on behalf of Chinese Chemical Society and Institute of Materia Medica, Chinese Academy of Medical Sciences.

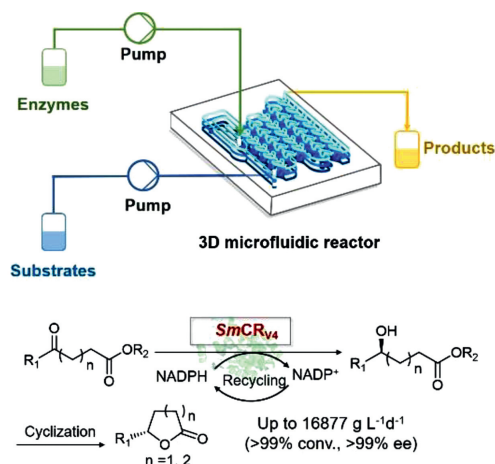
Biocatalysis combined with continuous-flow technology is a promising green manufacturing strategy for the pharmaceutical and fine-chemical industries [1,2]. The continuous-flow process carried out automatically in a microreactor can improve biocatalysis performance, making large-scale bioproduction more cost-effective due to significantly reduced reaction volume, improved mass transfer, shorter reaction time, and improved space-time yield [3,4]. The small size of the microreactors used in the continuous-flow process allows for precise manipulation of the reaction parameters. This facilitates process scale-up through parallel operation while avoiding issues caused by reactant mixing, substrate or product inhibition, and allosteric control [5]. Furthermore, the stability of biocatalysts is also improved because they are working in a laminar flow which is a mild environment without harsh stirring used in batch reactions.

Microfluidic chips have been widely used in continuous-flow technology over the last decade [6–10]. A variety of methods, such as photolithography [11,12], soft lithography [13–19], and nanoimprint lithography [20,21], have been used to fabricate microfluidic chips. The microfluidic channels are typically arranged on a two-dimensional (2D) plane in most chips. Although it is simple to construct these 2D microfluidic chips, the small interior area limits their reaction volume, and as a result, the residence time is unfavorable for enzyme catalysis since its reaction kinetics are slower than those of chemical catalysis. Therefore, the design and fabrication of three-dimensional (3D) microfluidic chips with a large specific surface area, smooth channel walls, and well-controlled 3D structures inside the chips are desirable. 3D chips can use their inner space more effectively, which increases reaction volume and residence time. Moreover, glass should be used in the fabrication of 3D microfluidic chips since it is more transparent, more tolerant to organic solvents, and has superior mechanical stability than polymers. Although the above-mentioned techniques, especially soft lithography, are quick and cost-effective, they cannot directly write 3D microfluidic structures on glass. In recent years,

* Corresponding author.

E-mail address: ybai@ecust.edu.cn (Y. Bai).

¹ These authors contributed equally to this work.



Scheme 1. The continuous-flow synthesis of optically pure (*R*)- γ -decalactone in a 3D microfluidic reactor.

femtosecond laser engraving technology has recently emerged as an ideal tool for precisely constructing 3D structures in glass substrates in a one-step continuous process [22–24]. Inspired by these advancements, we aimed to design and make a 3D microfluidic reactor using this technology for the continuous enzymatic synthesis of chiral lactones.

In the previous studies, we reported a new carbonyl reductase from *Serratia marcescens*, *SmCR*, for the asymmetric synthesis of (*R*)-(+)- γ/δ -decalactone [25] which are chiral flavors widely used in the food and cosmetic industries [26]. Then the specific activity of the variant *SmCR*_{V4} toward methyl 4-oxodecanoate (**1g**) was enhanced 86-fold compared with the wild-type enzyme by using directed evolution and the space-time yield (STY) of **3g** reached 1175 g L⁻¹ d⁻¹ in the batch reaction [27]. However, the STY meets its limit during the scaling up in batch because of the low solubility of substrates (long-chain fatty keto acids/esters) and the poor mixing in larger batch reactors. Here, we developed the continuous-flow enzymatic synthesis of (*R*)- γ -lactones in a 3D microfluidic reactor with unprecedented STY and excellent enantioselectivity compared with batch reaction (Scheme 1). Importantly, the reaction can run continuously and automatically for up to 6 h with high substrate conversion in scaled-up 3D microfluidic reactors, demonstrating its feasibility for reaction scale-up.

First, a three-layer microchannel was designed and fabricated in borosilicate glass (90 mm × 75 mm × 12 mm) by femtosecond laser (Fig. S1 in Supporting information). The streamlined microchannel is 175 mm long, 0.9 mm deep, and has a volume of 1.72 mL (Fig. 1a). The functional modules of the microreactor are composed of two inlets, one outlet, and a string of successive heart-shaped mixing units (Fig. 1b and Fig. S2 in Supporting information). Due to the presence of repeated heart-shaped mixing units, the flow was continuously split and converged, which can enhance the mixing of substrates and enzymes in the flow. For example, some heart-shaped microchannels were designed to increase the turbulent characteristics of the fluid and enhance the heat and mass transfer process. Gidde *et al.* compared several different shapes of micromixers and demonstrated that the heart-shaped mixer is the most effective micromixer due to the remarkable chaotic convection effect [28]. Lee *et al.* used a heart-shaped low-flow microreactor for the reaction process study and conducted efficient ozonolysis of quinoline and quinoline derivatives [29]. Novak *et al.* experimentally evaluated the performance of a heart-shaped microfluidic module for *Candida antarctica* lipase B-catalyzed isoamyl acetate synthesis in a two-liquid phase system and obtained the highest productivities in this microreactor [30].

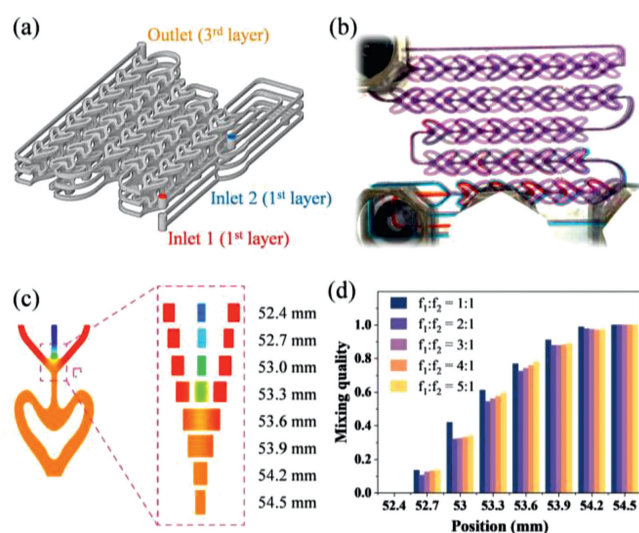


Fig. 1. Characterization of a 3D microreactor fabricated in borosilicate glass using femtosecond laser writing. (a) The top view of the microreactor design. (b) The blue ink and red ink were injected in the microreactor and mixed at 0.5 mL/min. (c) The concentration profiles at the beginning of the mixing process when the flow rate ratio of inlet 1 to inlet 2 is 5:1. The numbers indicate the positions of simulation points. (d) The corresponding mixing quality near the convergence point at different flow ratios (1:1, 2:1, 3:1, 4:1, 5:1), which was simulated by Fluent 2021R1. In all cases, the flow rate of inlet 2 was maintained at 1 mL/min and the flow rate of inlet 1 was increased from 1 mL/min to 5 mL/min.

To demonstrate the mixing effect in the microreactor, computational fluid dynamics (CFD) simulation was performed in the first heart-shaped mixing unit with the Fluent 2021R1 platform (Fig. 1c). The reactants 1 (red) and 2 (blue) were injected in the microreactor at 5 mL/min and 1 mL/min, respectively. At the converging point, the two species met and mixed. The mixing process was completed just before the entrance of the first mixing unit because the flow became homogeneous (orange). It should be noted that due to the higher flow rate of reactant 1, backflow was observed in flow 2 which gradually changed from blue to green, indicating the mixing happened before the converging point. To identify the flow field profile at the beginning of the mixing process, the velocity distribution at the confluence of three liquid flow paths was configured and the profiles showed the classic parabolic shape (Fig. S3 in Supporting information). To quantify the mixing process, the mixing quality at 8 positions in the mixing area from $z = 52.4$ mm to 54.5 mm was measured at different flow ratios (Fig. 1d). The mixing quality of 0 and 1 indicates no mixing and 100% mixing, respectively. As shown in Fig. 1d, the mixing quality gradually increased as mixing developed along the channel in different cases. At the front of the first heart-shaped entrance ($z = 54.5$ mm), the distribution of reactant in all cases was homogeneous and the mixing quality was equal to 1, which represented a good mixing effect. The mixing behavior in the mixing experiment at different flow rates agrees well with the corresponding simulation results (Fig. S4 in Supporting information). The mixing of the reactants was essentially completed when the flow ratio increased from 1:1 to 5:1, indicating the microreactor can provide a good mixing in a wide range of flow rates.

The catalytic activity of *SmCR*_{V4} was greatly affected by the reaction temperature in the asymmetric synthesis of **3g**. The enzyme activity of *SmCR*_{V4} toward **1g** was measured at different temperatures. The optimum temperature was 45 °C, at which it was 47% higher than at 30 °C (Fig. S5a in Supporting information). However, the reaction was performed at 30 °C in the batch reaction because of enzyme inactivation at 45 °C. The half-lives of *SmCR*_{V4} at 30 °C and 45 °C are 266 h and 26 h, respectively (Fig. S5b in Supporting

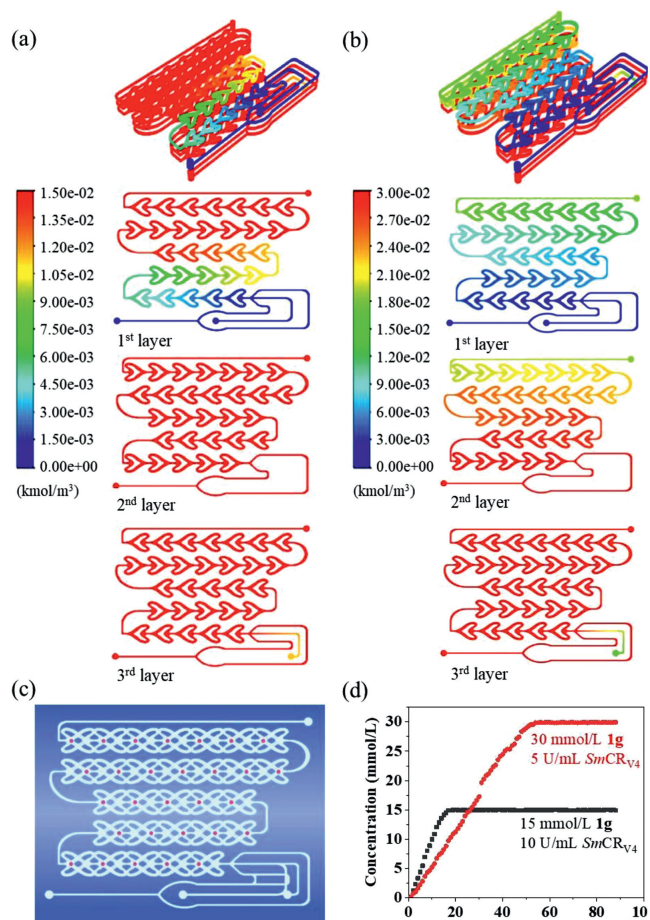


Fig. 2. The simulation of the enzymatic reactions in the 3D microfluidic reactor. The concentration profiles of **3g** in the whole microreactor, 1st layer, 2nd layer, and 3rd layer were plotted for cases 1 (a) and 2 (b), respectively. Simulation conditions: (a) 10 U/mL *SmCR_{v4}*, 15 mmol/L **1g**, 0.2 mmol/L NADP⁺, 100 mmol/L PBS (pH 7.0), 45 °C. The flow rates of substrate and enzyme were 1 mL/min. (b) 5 U/mL *SmCR_{v4}*, 30 mmol/L **1g**, 0.2 mmol/L NADP⁺, 100 mmol/L PBS (pH 7.0), 45 °C. The flow rates of substrate and enzyme were 3 and 1 mL/min. Sufficient NADPH recycling was ensured in both cases. Points were selected (c) to calculate the product concentrations (d) in the microreactor for cases 1 and 2.

information). In the microreactor, the residence time is very short (<20 min), greatly reducing the inactivation of the enzyme, so that the reaction can be carried out at the optimum temperature (45 °C). When the reaction temperature reached 45 °C, the conversion was the highest. Therefore, 45 °C was chosen as the working temperature for the following study (Fig. S6 in Supporting information).

To simulate the enzymatic reaction process in the 3D microfluidic reactor, a continuous-flow diffusion-reaction model was developed using the Fluent 2021R1 platform (Supporting information). The simulation was carried out with different flow rates to study the effect of reaction time on the catalytic process. Fig. 2a showed the concentration profiles of the product **3g** generated in the whole microreactor and in the 1st, 2nd, and 3rd layer microchannel, respectively (x-z plane, 3 mm, 6 mm, and 9 mm at y-axis). The value in the heat map (red) was 15 mmol/L, which was the maximum theoretical concentration of **3g** in a steady state because the initial substrate concentration was 15 mmol/L. It was found that the substrate was almost completely converted in the middle of the 1st layer microchannel and the conversion reached 99.5%. Then, the substrate concentration was increased to 30 mmol/L while the enzyme concentration was reduced, and



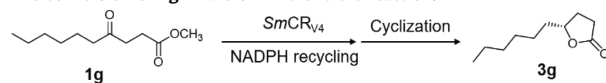
Fig. 3. Scale-up of the continuous-flow system. (a) The setup of 6 parallel microfluidic reactors. (b) The sample of optically pure **3g** was obtained as a light yellow liquid.

therefore, the substrate was nearly completely converted in the middle of the second layer channel (Fig. 2b). At the outlet, the final product conversion also reached 99.5%, indicating that the residence time was enough for the enzymatic reaction. To quantify the reaction process, 87 points (red points) were selected in the microchannel (Fig. 2c), and the product concentration at each point was calculated and plotted in Fig. 2d. Clearly, the concentration of **3g** gradually increased along the channel and the conversion reached >99% in each case. The simulation results indicated that the 3D microfluidic reactor had not been fully exploited at the substrate concentration of 30 mmol/L because the conversion reached 99.5% before the third layer. Thus, in theory, the conversion of the substrate at higher concentrations with the same amount of enzyme is possible by fully utilizing the third layer microchannel.

Subsequently, we converted **1g** in the 3D microfluidic reactor to experimentally evaluate the continuous-flow process's productivity (Table 1). First, the total activity of *SmCR_{v4}* and the residence time were maintained at 10 U/mL and 52 s, respectively. As the substrate concentration increased from 2 mmol/L to 15 mmol/L, the STY increased from 565 g L⁻¹d⁻¹ to 4238 g L⁻¹d⁻¹, which already exceeded the best STY (1175 g L⁻¹d⁻¹) [27] of the batch reaction (entries 1–3). Then, the flow rate ratio of **1g** to *SmCR_{v4}* was increased from 1.5:1 to 2.5:1, and the total activity of *SmCR_{v4}* decreased from 8 U/mL to 5.7 U/mL while the substrate concentration increased to 25 mmol/L (entries 4–6). Although the residence time decreased from 52 s to 30 s, the substrate conversions all reached >99% and the STY was enhanced to 12,279 g L⁻¹d⁻¹. Finally, we increased the substrate concentration to 30 mmol/L and found that >99% substrate was still converted within only 26 s (entry 7). The STY for the production of **3g** was as high as 16,877 g L⁻¹d⁻¹, which was the highest reported so far and 14.4 times higher than the best STY of the batch reaction. The conversions of 15 mmol/L and 30 mmol/L **1g** in entries 3 and 7 agreed well with the simulation results of Fig. 3, verifying the powerful capacity of the 3D microreactor in continuous-flow enzymatic reactions.

The substrate concentration of 30 mmol/L has already reached the solubility limit of **1g** because 10% (v/v) dimethyl sulfoxide (DMSO) was added as a co-solvent in the phosphate buffer (100 mmol/L, pH 7.0) to improve the substrate solubility. In addition, due to the excellent thermal stability of *SmCR_{v4}* and the short resident time in the continuous-flow reaction, *SmCR_{v4}* retained its original catalytic properties after the continuous-flow reaction (Fig. S7 in Supporting information).

Although the simulation result indicated that the conversion of **1g** at higher concentrations is theoretically possible, the substrate concentration was not further increased due to the limit of DMSO in the reaction system. To further compare the performance of the continuous flow and the batch reaction, the conversion of **1g** was carried out under the same conditions in the 3D microfluidic and batch reactor. As shown in Fig. S8 (Supporting information), con-

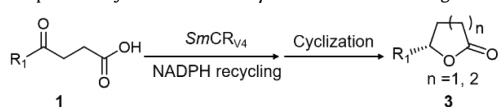
Table 1
The conversion of **1g** in the 3D microfluidic reaction.^a

Substrate 1g (mmol/L)	<i>SmCR</i> _{v4} (U/mL)	<i>f</i> _S : <i>f</i> _E ^b	Time (s)	Conv.(%)	STY ^c (g L ⁻¹ d ⁻¹)	<i>ee</i> (%)
2	10	1:1	52	>99	565	97 (R)
10	10	1:1	52	>99	2828	97 (R)
15	10	1:1	52	>99	4238	97 (R)
18	8	1.5:1	42	>99	6355	97 (R)
20	6.7	2:1	35	>99	8420	97 (R)
25	5.7	2.5:1	30	>99	12,279	97 (R)
30	5	3:1	26	>99	16,877	97 (R)

^a Reaction conditions: glucose (1.5 equiv. of **1g**), NADP⁺ (0.2 mmol/L), *BmGDH* (2 mg/mL), sodium phosphate buffer (100 mmol/L, pH 7.0), 45 °C.

^b Flow rate ratios of the substrate to the enzyme (mL/min).

^c Space-time yield.

Table 2
Preparative synthesis of chiral γ - and δ -lactones using keto acids.^a

Product	<i>SmCR</i> _{v4} (mU/mL)	Conv. (%)	<i>ee</i> (%)
(3a)	59	86	96 (R)
(3b)	131	>99	99 (R)
(3g)	254	>99	97 (R)
(3d)	247	>99	95 (R)
(3e)	96	>99	99 (R)
(3f)	54	>99	97 (S)

^a Reaction conditions: Substrate (2 mmol/L), glucose (3 mmol/L), NADP⁺ (0.2 mmol/L), *BmGDH* (2 mg/mL), sodium phosphate buffer (100 mmol/L, pH 7.0), 45 °C. The residence time was 20 min.

versions of >99% were achieved within 12.5 and 12 min at 30 °C and 45 °C in the microreactor, respectively. However, the same conversions were obtained at 30 min in the batch reactor.

To explore the scope of this new continuous-flow strategy for the synthesis of optically pure lactones, a variety of keto acids were subjected to the general experimental conditions established in the 3D microfluidic reactor (Table 2). Most of the lactones were obtained with excellent conversions (>99%) and enantioselectivity (>99% *ee*) within 20 min except for the reduction of **1a** whose conversion decreased to 86%. The longer residence time was attributed to the relatively lower activity of the enzyme toward these substrates than **1g** (Table S1 in Supporting information). However, the STYs of these chiral lactones were all higher than those obtained in the batch reactions [27]. Therefore, further improvement of the continuous-flow system could be achieved with the directed evolution of enzymes.

The high stability of *SmCR*_{v4} (*t*_{1/2} = 26 h at 45 °C) makes it possible to recycle and reuse the enzyme considering that its working time was 1–20 min in the 3D microreactor, which is desirable in terms of operation cost and sustainable manufacturing. To recy-

cle the enzyme, the collected product solution was re-pumped into the microreactor continuously as the enzyme stock solution for the enzymatic reactions. This enzyme-recycling continuous system run steadily for 5 h, and the substrate conversion was always >97% at different time (Fig. S9 in Supporting information). Furthermore, the reaction samples were taken and the catalytic performance of *SmCR*_{v4} was compared by measuring the conversion of 4 mmol/L substrate (Fig. S10 in Supporting information). It was found that the enzyme's catalytic capability remained stable throughout the 5 h, which validated the feasibility and reliability of enzyme recycling in the continuous-flow biocatalysis reactions due to the high stability of *SmCR*_{v4}.

The scale-up process is essential to the industrial application of continuous flow processes, which can increase working volumes and further improve total productivity. By controlling the same experimental conditions and the same residence time, it is possible to reproduce the experimental results in larger parallel or cascade microreactors. Different from the volume scale-up of batch reactions, the continuous-flow process can realize large-scale production by running multiple microreactors in parallel or cascade. With more microreactors connected online, productivity can be expanded from the gram level to the kilogram level, which can save scale-up time and cost significantly [17]. Production on the order of kg/min can be readily achieved by running tens of modular reaction units [31]. Gustafsson *et al.* demonstrated the advantages of using continuous-flow processing at the scaled-up production of an inhibitor intermediate, which reduced the costs of materials and improved product quality [32].

To demonstrate the scale-up feasibility and the operation stability of the 3D microfluidic reactor, six larger microfluidic reactors (total 65 mL working volume) were connected in cascade and the continuous-flow reaction was operated automatically for 6 h at a flow rate of 20 mL/min which was much higher than 2 mL/min in the lab setup (Fig. 3a). Here, the scale-up principle is to keep the residence time in each microreactor (32 s) similar to that (26 s) in the lab experiments. Remarkably, the system remained stable without leakage for 6 h and the substrate conversions were all >99% during the whole process (Fig. S11 in Supporting information). Finally, optically pure **3g** (>99% *ee*) was obtained with 83% yield after separation and purification (Fig. 3b). It is noteworthy that the microchannel configuration of the larger 3D microreactors was not heart-shaped, so the residence time was a little bit longer than that in the lab microreactor. However, the working flow rate was increased from the typical 2 mL/min of lab experiments to 20 mL/min, and the total working flow was increased from 1.72 mL to 65 mL, significantly enhancing the capacity of substrate processing while keeping the same conversions (>99%). In fact, thanks to the 3D microchannel set up in a single chip, it is possible that the residence time can be readily optimized later by adjusting flow

rates according to the cost of substrate and enzyme, providing a flexible production module for different productivity requirements.

In conclusion, we designed and developed a 3D microreactor using femtosecond laser technology, which was used as an efficient platform for the continuous-flow synthesis of chiral γ - and δ -lactones. The effectiveness of this process was demonstrated in the synthesis of **3g** with a residence time as short as 26 s and space-time yield up to 16,877 g L⁻¹ d⁻¹, which was 14.4 times higher than that of the best batch process. The high efficiency of this system was due to the enhanced mixing efficiency of the 3D microfluidic reactor and the high activity and stereoselectivity of the enzymatic reaction. As a result of the enzyme recycling and the easy scale-up of the microfluidic system demonstrated in this work, the combination of biocatalysis and continuous-flow technology not only leads to significant reductions in reaction time and increased productivity, but can be also considered a sustainable technology for the production of fine chiral chemicals used in various industries.

Declaration of competing interest

The authors declare that they have no known competing financial interests or personal relationships that could have appeared to influence the work reported in this paper.

Acknowledgments

This work was financially sponsored by the National Key Research and Development Program of China (No. 2021YFC2102804) and the National Natural Science Foundation of China (No. 22078096).

Supplementary materials

Supplementary material associated with this article can be found, in the online version, at doi:10.1016/j.ccl.2023.108684.

References

- [1] C. Jiménez-González, P. Poehlauer, Q. Broxterman, et al., *Org. Process Res. Dev.* 15 (2011) 900–911.
- [2] W. Luo, F. Liu, Y.H. Guo, et al., *Chin. Chem. Lett.* 34 (2023) 107636.
- [3] Y. Wu, W.Q. Chen, Y.Q. Zhao, et al., *Chin. Chem. Lett.* 26 (2015) 334–338.
- [4] Y.J. Hu, J. Chen, Y.Q. Wang, et al., *Chem. Eng. J.* 437 (2022) 135400.
- [5] C. Wiles, P. Watts, *Green Chem.* 14 (2012) 38–54.
- [6] R. Gopi, V. Thangarasu, A. Vinayakselvi M, A. Ramanathan, *Renew. Sust. Energ. Rev.* 154 (2022) 111869.
- [7] J.M. Bolivar, D. Valikhani, B. Nidetzky, *Biotech. J.* 3 (2019) 1800244.
- [8] V. Hakke, S. Sonawane, S. Anandan, et al., *Nanomaterials* 11 (2021) 1–21.
- [9] J. Ren, K. Niu, M. Wu, et al., *Chin. Chem. Lett.* 34 (2023) 107985.
- [10] R. Wohlgemuth, I. Plazl, P. Žnidaršič-Plazl, et al., *Trends Biotech* 33 (2015) 302–314.
- [11] K. Kusakabe, S. Morooka, H. Maeda, *Korean J. Chem. Eng.* 18 (2001) 271–276.
- [12] R.J. Hu, M. Lei, H.S. Xiong, et al., *Tetrahedron Lett.* 49 (2008) 387–389.
- [13] C. Chande, N. Riaz, V. Harbour, et al., *Technology (Singap. World Sci)* 8 (2020) 50–57.
- [14] C.F. Carlborg, T. Haraldsson, K. Öberg, et al., *Lab Chip* 11 (2011) 3136–3147.
- [15] M. Srisa-Art, S.D. Noblitt, A.T. Krummel, et al., *Analy. Chim. Acta* 1021 (2018) 95–102.
- [16] B. Mondal, S. Pati, P.K. Patowari, *Mater. Today: Proceed* 26 (2020) 1271–1278.
- [17] J.M. Burke, K.R. Pandit, J.P. Goertz, et al., *Biomicrofluidics* 8 (2014) 056503.
- [18] F. Qian, Z. He, M.P. Thelen, et al., *Bioresource Tech.* 102 (2011) 5836–5840.
- [19] J. Love, J.R. Anderson, G.M. Whitesides, *MRS Bulletin* 26 (2001) 523–528.
- [20] S. Li, A. Kazemi-Moridani, Y. Zhou, et al., *ACS Appl. Mater. Interfaces* 10 (2018) 8173–8179.
- [21] L.M. Cox, A.M. Martinez, A.K. Blevins, et al., *Nano Today* 31 (2020) 100838.
- [22] J. Xu, X. Li, Y. Zhong, et al., *Adv. Mater. Techn.* 3 (2018) 1800372.
- [23] W. Li, W. Chu, D. Yin, et al., *Appl. Phys. A* 126 (2020) 816.
- [24] A. Zhang, J. Xu, X. Li, et al., *Sensors* 22 (2022) 1124.
- [25] C. Zhang, J. Pan, C.X. Li, et al., *Catal. Commun.* 102 (2017) 35–39.
- [26] A. Drożdż, U. Hanefeld, K. Szymańska, et al., *Catal. Commun.* 81 (2016) 37–40.
- [27] M. Chen, X.Y. Zhang, C.G. Xing, et al., *ChemCatChem* 11 (2019) 2600–2606.
- [28] R.R. Gidde, P.M. Pawar, H.S. Santana, *Int. J. Chem. Reactor Eng.* 21 (2023) 181–192.
- [29] K. Lee, H. Lin, K.F. Jensen, *React. Chem. Eng.* 2 (2017) 696–702.
- [30] U. Novak, D. Lavric, P. Žnidaršič-Plazl, *J. Flow Chem.* 6 (2016) 33–38.
- [31] G.S. Calabrese, S. Pissavini, *AIChE. J.* 57 (2011) 828–834.
- [32] T. Gustafsson, H. Sörensen, F. Pontén, *Org. Process Res.* 16 (2012) 925–929.